Available online at www.sciencedirect.com

jmr&t Journal of Materials Research and Technology

journal homepage: www.elsevier.com/locate/jmrt

Original Article

Two step–ageing of 7xxx series alloys with an intermediate warm-forming step

Johannes A. Österreicher [a,*], Florian Grabner [a], Matheus A. Tunes [b], Diego S.R. Coradini [b], Stefan Pogatscher [b], Carina M. Schlögl [a]

[a] LKR Light Metals Technologies, Austrian Institute of Technology, Lamprechtshausenerstraße 61, 5282 Ranshofen, Austria

[b] Chair of Nonferrous Metallurgy, Department of Metallurgy, Montanuniversitaet Leoben, Franz-Josef-Straße 18, 8700 Leoben, Austria

ARTICLE INFO

Article history:
Received 10 December 2020
Accepted 14 March 2021
Available online 21 March 2021

Keywords:
Aluminium alloy
Automotive
Retrogression
Paint-bake
Deep-drawing
Transmission electron microscopy

ABSTRACT

Two-step ageing of 7xxx series alloys can reduce ageing time while obtaining similar mechanical properties as a longer isothermal heat treatment. In this paper, an intermediate deep-drawing step at 120–160 °C is introduced to produce elongated cup–shaped parts with near-T6 strength. A Cu-containing (Alclad 7075) and a non-standard low-Cu alloy (7021+) are used. Formability and the final mechanical properties after various second ageing steps are reported. Hardening precipitates are studied by means of transmission electron microscopy and differential scanning calorimetry. We found that the pre-aged 7021+ alloy can be deep-drawn at lower temperature (120 °C) than pre-aged Alclad 7075 (160 °C). Both alloys respond well to the two-step ageing regime with the parts achieving up to 99% and 98% of the T6 yield strength of Alclad 7075 and 7021+, respectively. Compared to T6, the distribution of hardening nanoscale Mg–Zn-precipitates is slightly coarser after two-step hardening regimes with intermediate warm-forming. Mechanical properties are closest to T6 for a final ageing step at 165 °C for 130 min and coarsening of hardening precipitates is less pronounced compared to a simulated paint-bake cycle (185 °C, 34 min).

1. Introduction

For artificially peak-ageing 7xxx series alloys, a heat treatment at 120 °C for 24 h is generally considered the reference method [1]. It leads to a fine distribution of nanoscale hardening precipitates such as Guinier–Preston zones (GP zones) and η′ precipitates [2–4]. However, the long duration of such a treatment is not always desirable for industrial purposes. Therefore, multi-stage heat treatments have been suggested for reaching similar mechanical properties in less time [5–7]. These treatments rely on a first low temperature step to create a fine distribution of GP zones and a second step at a higher temperature that aims to complete precipitation [7,8]. In the automotive industry, this second step can be carried out using the paint-bake treatment for curing the paint. In a recent

* Corresponding author.
E-mail address: johannes.oesterreicher@ait.ac.at (J.A. Österreicher).
https://doi.org/10.1016/j.jmrt.2021.03.062

Table 1 – Chemical composition in weight percent (wt.%).

	Si	Mg	Mn	Fe	Cu	Cr	Zn	Zr	Al
7021+	0.21	2.27	0.01	0.04	0.21	0.01	5.67	0.12	91.4
7075 (base)	0.06	2.28	0.04	0.09	1.26	0.19	5.51	-	90.5

study for AA7075 [4], we showed that by combining pre-ageing and a paint-bake treatment with an intermediate warm-forming step, ~95% of T6-level strength can be reached. Furthermore, non-isothermal heat treatments can lead to better stress corrosion cracking (SCC) resistance due to the coarsening of grain boundary phases [3,9].

For Cu-containing 7xxx series alloys, Sha et al. [10] reported that transformation of Cu-containing small GP-I zones (<30 solute atoms) into η′ is the dominant mechanism for η′ formation during isothermal ageing at 121 °C. Lee et al. [7] found that for this transformation to take place at a paint bake temperature of 180 °C, the GP zones need to be grown larger than a critical size to be more temperature-stable. In contrast, pre-ageing of a near Cu-free 7xxx series alloy was found to have no significant influence on subsequent paint bake response at 185 °C [6].

Harrison et al. [11] reported a shortened multi-step treatment to reach essentially peak-aged strength in AA7075 and AA7085 alloys, referred to as "short-T6" in the following. This heat treatment consists of solution heat treatment and quenching, a 24 h–long natural ageing interval, and artificial ageing at 110 °C for 2 h followed by 165 °C for 2 h. The investigation allowed Harrison et al. to shed new insights into industrial paint-bake cycles.

The effects of natural ageing on subsequent artificial ageing of Al–Zn–Mg alloys are subject to current discussion. It has been reported that 72 h of natural ageing combined with pre-ageing can inhibit secondary natural ageing [12]. In

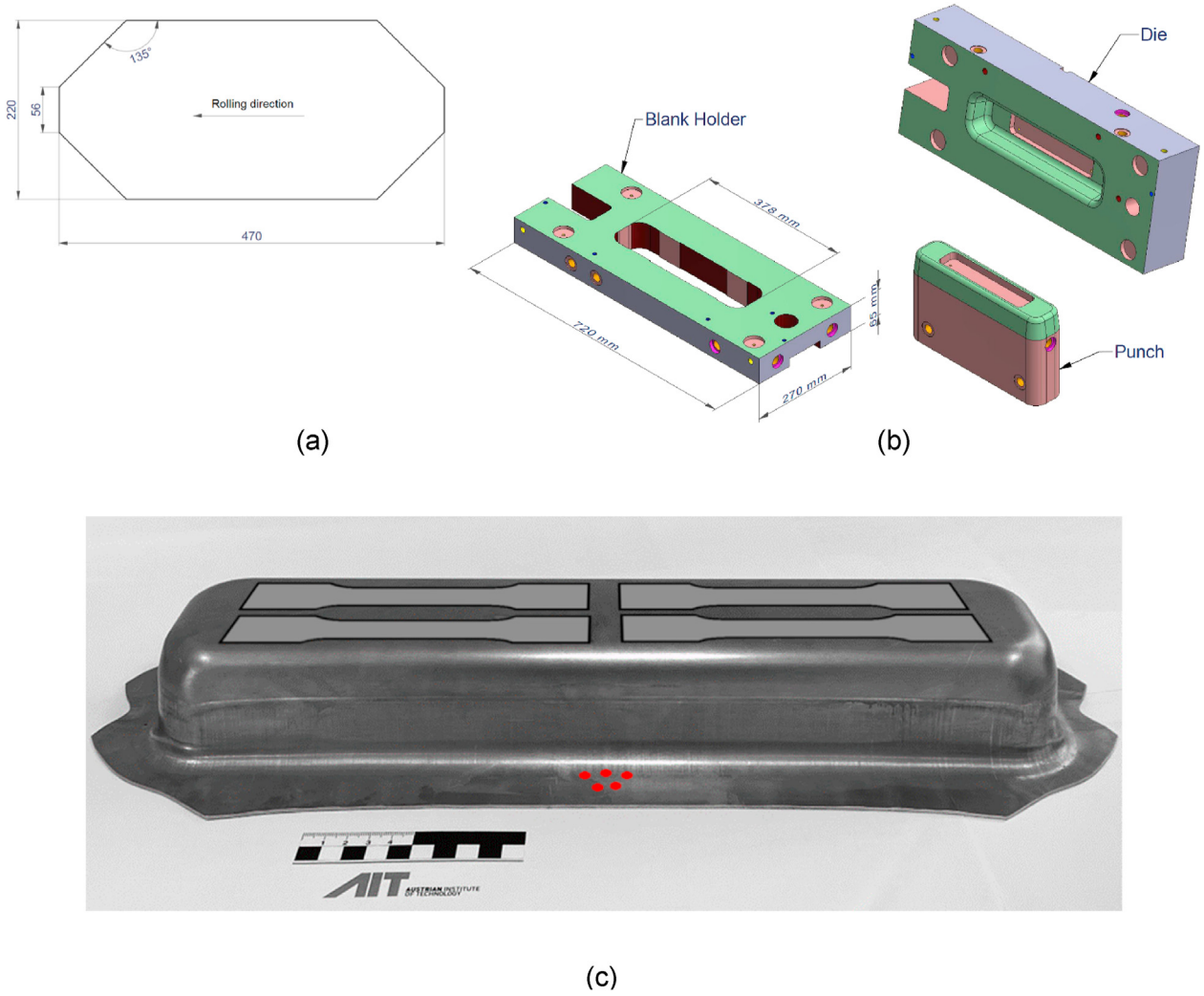

Fig. 1 – (a) Blank dimensions in mm, (b) drawing of the deep-drawing tool, and (c) final part with schematic indication of sampling locations for tensile testing (dumbells) and DSC analysis (red dots).

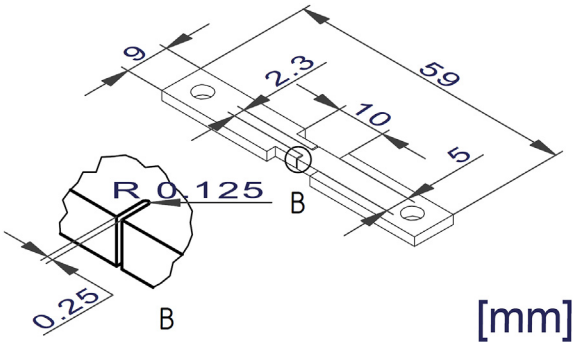

Fig. 2 – Miniaturized notched tensile tests for testing at RT and warm-forming temperatures.

another work, 24 h of natural ageing after retrogression were introduced in a retrogression and re-ageing (RRA) process to achieve high strength and stress corrosion cracking (SCC) resistance [13]. With regards to paint-bake response, no significant influence of a week of natural ageing was found in [6]. Either way, in industrial settings, natural ageing intervals are often hard to avoid and allowing for some natural ageing can make a process chain easier to adopt.

In this study, we investigate the compatibility of the two-step short-T6 heat treatment with an intermediate warm-forming step [11] for two 7xxx series alloys, differing in Cu content. Moreover, a simulated paint-bake treatment is carried out instead of the last ageing step of the short-T6 treatment.

2. Materials and methods

We used rolled sheet of Alclad 7075 (O temper, 1.4 mm) and 7021+ (F temper, 1.5 mm), both obtained from AMAG rolling GmbH. 7021+ is a non-standard alloy based on AA7021 with increased Mg and Zn levels. The chemical compositions, measured using a Spectromaxx 6 device (Spectro Analytical Instruments), are given in Table 1. The estimated measurement uncertainty is <2.5% of the measured value. Trace elements not given in Table 1 were <0.1 wt.% in total for either alloy.

Blanks with the dimensions given in Fig. 1 (a) were cut. Solution heat treatment (SHT) was performed by placing the

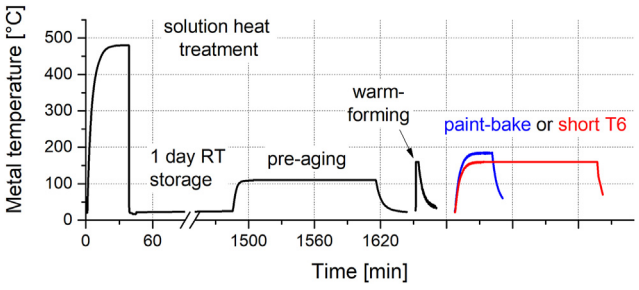

Fig. 3 – Time/temperature schematic of the whole process chain. The figure shows solution heat treatment conditions for Alclad 7075.

blanks in a pre-heated oven (AA7075: 480 °C, 25 min; AA7021+: 515 °C, 15 min) followed by quenching in water. After one day (24 h) of natural ageing, the blanks were placed in an oven pre-heated to 110 °C for 2 h [11] and subsequently allowed to cool to room temperature (RT) at ambient air.

RT and warm notched tensile tests were conducted in triplicate using a Bähr DIL 805 A/D deformation dilatometer. Specimens of the geometry given in Fig. 2 were cut in rolling direction from pre-aged sheet (heat treatment as described above). For the warm notched tensile tests, the specimens were heated at a rate of 20 K/s to 120 or 160 °C and held at this temperature until 30 s after the beginning of heating; then, deformation was started at a strain rate of 0.006 s^{-1} or 1 s^{-1}. The heating and soaking regime was chosen to simulate contact heating of the blanks in the blank holder before deep-drawing [4]. The obtained force/displacement-curves were well reproducible and thus, averaged curves are reported here. However, data for force levels <600 N was removed and extrapolated with a constant inclination due to displacement measurement instability in this region.

For deep-drawing, the blanks were lubricated using Zeller + Gmelin Multidraw Drylube E1 and placed in a pre-heated blank holder (120 or 160 °C). Punch and die were also pre-heated to the desired temperature. A drawing of the tool is given in Fig. 1 (b). Heating of the tool parts was accomplished by electrical resistance heating and controlled using thermocouples embedded in the tools and a Profitemp hot runner controller (PSG Plastic Service GmbH). The blank holder was closed with 50 kN (~25 bar) and after 30 s, deep-drawing was started at a speed of 20 mm/s. The draw depth was ~50 mm. A 160 t double-sided hydraulic press was used (Walter Neff GmbH).

The formed parts were either subjected to a simulated paint-bake treatment at 185 °C for 34 min or to the short-T6 treatment at 165 °C for 130 min (furnace time). A schematic of the whole process chain is given in Fig. 3. As a comparison, unformed sheets were artificially aged to T6 condition (120 °C for 24 h) after solution heat treatment and quenching (as above).

Tensile specimens ($L_0 = 50$ mm) taken from the parts (Fig. 1 c) were measured in quadruplicate at RT according to EN-ISO 6892-1 B using a Zwick Z250 materials testing machine. Tensile specimens taken from the T6 sheet material (not deep-drawn) was performed in the same way but using five specimens per alloy.

For differential scanning calorimetry (DSC), samples with a diameter of 3 mm were punched from the sheet or parts (Fig. 1 c), deburred using sand paper, and cleaned in isopropanol. The samples were placed in a Al_2O_3 crucible and measured in a nitrogen atmosphere (99.999 vol. % purity, 50 ml/min) using a Netzsch DSC 204 F1 calorimeter at a heating rate of 10 °C/min up to 550 °C. Two samples were measured to ensure reproducibility; only one curve per condition is shown in this paper. The obtained curves were baseline-corrected by subtracting a pure Al (99.98%) curve and subsequently manually fitting a linear function of the form $y = kx + d$ to the peak-free regions at 100–130 °C and around 470 °C to remove remaining contortion similar to the approach described by Osten et al. [14].

For transmission electron microscopy (TEM), samples were taken in the same region as the DSC samples (Fig. 1 c) or from

Table 2 – Strength of the parts compared to T6 sheet reference. Error values represent standard deviation of five (T6) or four (other tempers) tensile specimens.

	Alclad 7075		7021+	
Temper	YS [MPa]	UTS [MPa]	YS [MPa]	UTS [MPa]
T6 (24 h, 120 °C)	456.2 ± 1.3	515.3 ± 1.3	441.5 ± 1.4	482.3 ± 0.7
Pre-aged, warm-formed + short-T6	453.4 ± 3.0	506.1 ± 2.7	433.5 ± 1.3	459.6 ± 1.5
Pre-aged, warm-formed, + "paint-bake"	445.2 ± 0.4	500.9 ± 0.3	406.3 ± 0.6	438.2 ± 0.6

heat-treated sheet and ground to a thickness of 100 μm. Discs with 3 mm diameter were mechanically punched and subsequently subjected to jet electropolishing (JEP) to electron-transparency. JEP was performed with an applied electric potential of 12 V at 263 K until perforation. A 1/3 nitric acid and 2/3 methanol electrolyte solution was used. After JEP, the samples were washed by immersing them ten times into each of three subsequent pure methanol baths; the samples were left to dry in air. A Thermo Scientific Talos F200X scanning transmission electron microscope (STEM) was used for microstructural characterization. The microscope operates a field emission gun filament at 200 keV and for the characterization reported in this work, energy dispersive X-ray (EDX) spectroscopy was used in the STEM mode.

3. Results and discussion

Deep-drawing without cracks was possible for pre-aged 7021+ at 120 °C and for both pre-aged alloys at 160 °C. Attempts to deep-draw the pre-aged material at lower temperatures than 120 or 160 °C, for 7021+ and Alclad 7075, respectively, were not successful due to cracking.

To study the failure behavior of the pre-aged material during forming, we performed notched tensile tests at the various forming temperatures and two different strain rates. Notched tensile specimens were used to investigate the plane strain condition, which is critical during deep-drawing [15,16]. A preliminary finite element method (FEM) investigation showed that occurring strain rates are $<1s^{-1}$, with many elements experiencing only quasi-static strain. Thus, the warm notched tensile tests were performed at quasi-static conditions (0.006 s^{-1}) and at a strain rate of 1 s^{-1}; the results are given in Fig. 4. In general, higher temperatures lead to lower force levels and higher elongation at break. The increase in elongation with temperature is especially pronounced for Alclad 7075 in the quasi-static condition. At the higher strain rate (1 s^{-1}), the increase in elongation compared to RT is much stronger for 160 than 120 °C. Since cracks during deep-drawing occur in region with high strain (and thus, high strain rates), this finding could explain why Alclad 7075 depends on the higher temperature for successful deep-drawing.

A complex interplay of introduction of lattice defects, dynamic recovery, and precipitation of hardening phases occurs during warm-forming of age-hardenable alloys. At the higher strain rate, there is less time for dynamic recovery to take place, which can explain higher work hardening rates and reduced elongation. This strain rate sensitivity is more pronounced for Alclad 7075 and could be related to the stimulation of GP-Zone precipitation during the pre-ageing step and the higher thermal stability of Cu-containing precipitates, providing more resistance to dislocation movement [17–19].

The mechanical properties of the warm-formed and artificially aged parts are given and compared to T6 in Fig. 5.

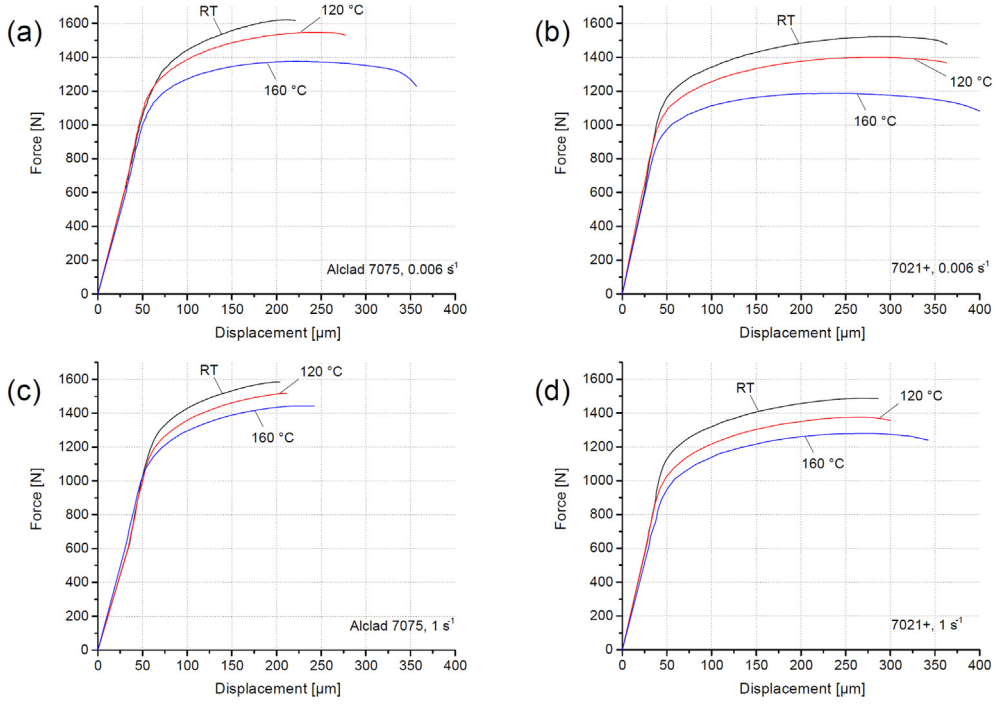

Fig. 4 – Force/displacement curves of miniaturized notched tensile tests of the pre-aged temper at RT and forming temperatures. (a) Alclad 7075, 0.006 s^{-1}, (b) 7021+, 0.006 s^{-1}, (c) Alclad 7075, 1 s^{-1}, and (d) 7021+, 1 s^{-1}.

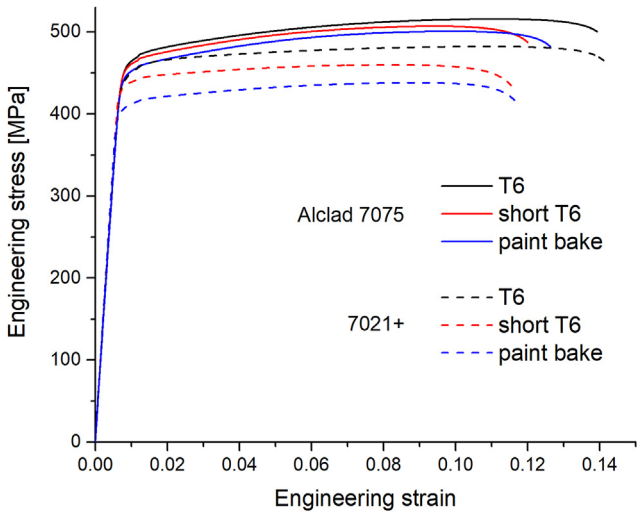

Fig. 5 – Averaged stress/strain curves of the pre-aged, warm-formed (160 °C), and artificially aged parts (short-T6 and paint-bake) compared to T6 sheet.

Additionally, yield strength (YS) and ultimate tensile strength (UTS) values are given in Table 2.

For 7021+, the short-T6 treatment in combination with warm-forming (160 °C) resulted in 98% of the YS compared to the reference T6 material aged for 24 h. UTS and elongation were 95% and 83% of the reference, respectively. The pre-aged, warm-formed (160 °C) and paint-baked 7021+ achieved 92% of the YS, 91% of the UTS, and 83% of the elongation compared to T6.

The mechanical properties after artificial ageing of the 7021+ parts deep-drawn at 120 °C were essentially the same as for the parts deep-drawn at 160 °C, shown in Fig. 5. This can be explained by the short duration of the deep-drawing process relative to both artificial ageing processes.

For Alclad 7075, the shortened T6 treatment in combination with warm-forming (160 °C) resulted in 99% of the YS compared to the reference T6 material aged for 24 h. UTS and elongation were 98% and 87% of the reference, respectively. The pre-aged, warm-formed (160 °C) and paint-baked Alclad 7075 achieved 98% of the YS, 97% of the UTS, and 92% of the elongation of the T6 reference aged for 24 h.

Since the YS is an important design value for most technical applications, the shortened T6 treatment is an attractive alternative to the time-consuming reference T6 treatment for both investigated alloys. An almost identical strength level can be achieved at the expense of a roughly 15% lower elongation. Such pre-ageing could be performed already at the rolling mill, thus eliminating solution heat treatment and quenching procedures at the parts manufacturer.

In order to further assess the short-T6 treatment, DSC investigations were carried out. In Fig. 6, DSC curves of Alclad 7075 and 7021+ are given in the various tempers. In accordance with [4,20–24], the peaks can be interpreted as follows: The endothermic peak 1 is likely linked to the reversion of GP zones and η′. The exothermic doublet 2a and 2 b for Alclad 7075 is potentially associated with the transformation of η′ to η (2a) and formation of η (2 b). In 7021+, these peaks are combined into a single peak 2, which is typical for low-Cu alloys as reported in [19,24].

For both alloys, the dissolution peak 1 is shifted to the right for the short-T6 treatment compared to T6, and even more for the paint-baked samples, indicating coarsening of the precipitates, which is in good agreement with earlier work [4]. Furthermore, peak 1 and peaks 2/2a/2 b are lower in amplitude, which could mean that the transformation from GP zones to η′ (and maybe also from η′ to η) may have started before the DSC measurements.

The microstructure of AA7075 after warm-forming at various temperatures and paint-bake has been investigated by TEM in a previous work [4]. Despite very similar mechanical properties, the distribution of hardening Mg–Zn-precipitates was coarser than in the T6 state. Analogously, Fig. 7 gives a comparison of 7021+ in the different tempers studied in this work. Again, the precipitate structure of the warm-formed and paint-baked temper is coarser than in T6, a finding which is in good agreement with the DSC results (Fig. 6). In contrast to AA7075 [4], this coarser precipitate structure leads to a stronger decline in strength (Fig. 5). This could indicate the occurrence of a shearable–non-shearable transition of at least parts of the hardening precipitates, resulting in lower strength [25,26]. The precipitate structure of the warm-formed parts in the short-T6 temper is finer than in the paint-baked condition, but not as fine as in T6. This corresponds well to the

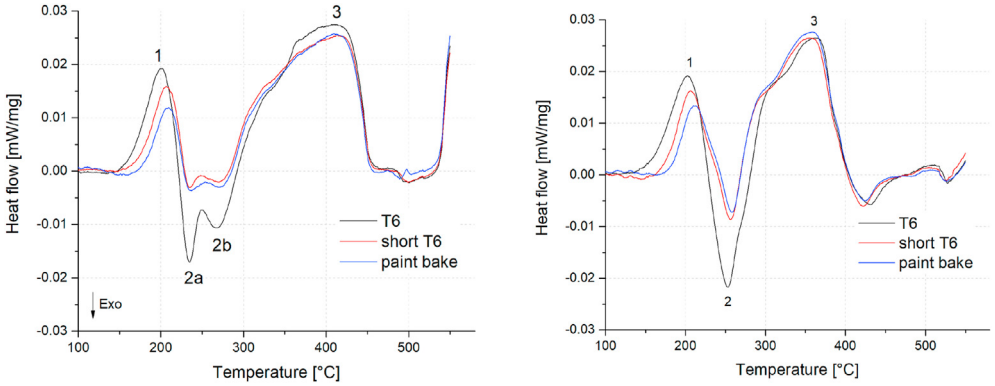

Fig. 6 – DSC curves of Alclad 7075 (left) and 7021+ (right) in T6, warm-formed plus short-T6, and warm-formed plus paint baked tempers. A shift of peak 1, linked to the reversion of GP zones and η′, to higher temperatures is likely due to coarser precipitation of these phases.

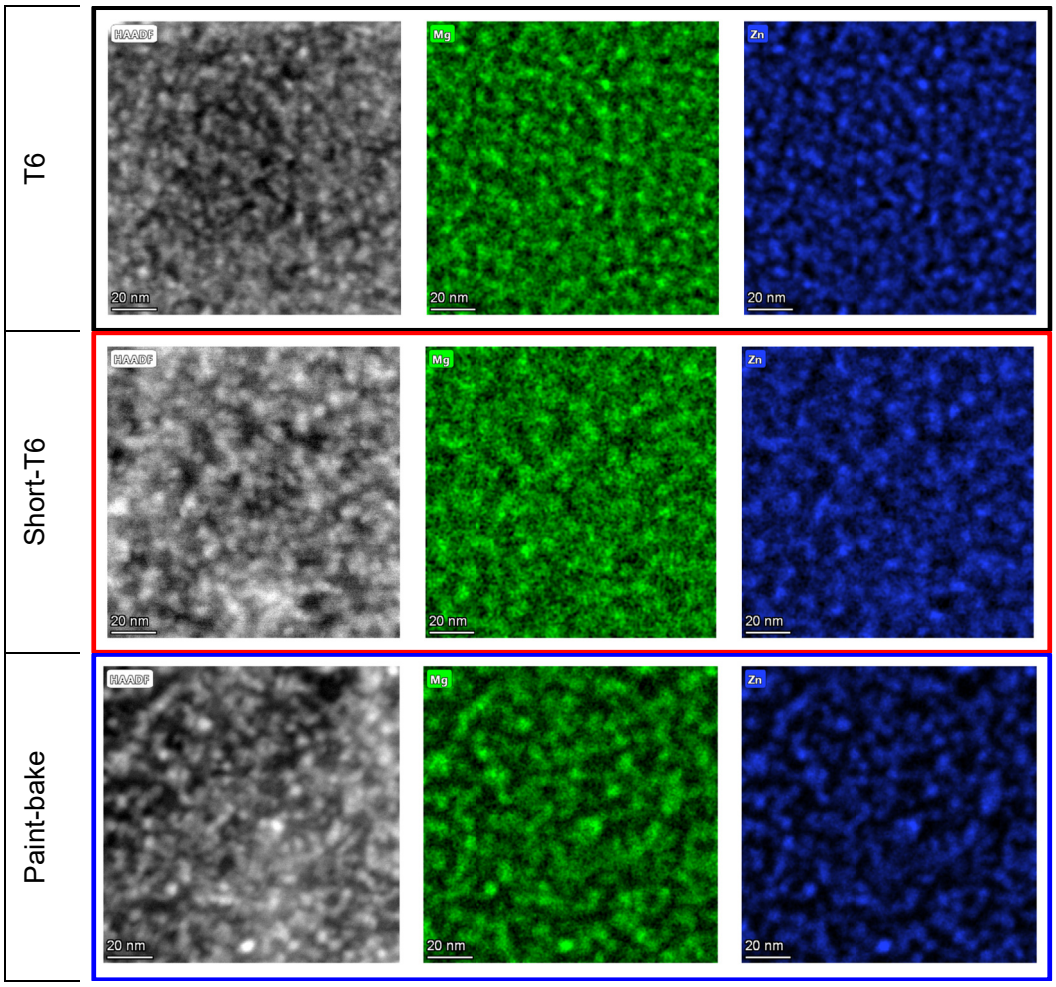

Fig. 7 – STEM-HAADF micrographs and EDX maps of AA7021+ in T6, warm-formed plus short-T6, and warm-formed plus paint bake tempers. The hardening Mg–Zn-precipitates are coarser for the two-step hardening regimes, likely due to the higher ageing temperatures.

mechanical properties exhibited in Fig. 5, which are better than in paint-baked state, but slightly worse than in T6. The better suitability of Alclad 7075 for the two-step ageing treatments investigated here might be due to Cu enhancing the precipitation of GP-zones and higher stability of Cu-containing GP zones during the second, high-temperature heat treatment step [7,18,23,24,27]. Related, in [4], a slight negative effect of warm-forming was found when carried out at 250 °C, but not at 230 °C or lower temperatures.

In the automotive industry, extra artificial ageing of parts before assembly of the body-in-white is not desired; the artificial ageing should be accomplished simultaneously with the hardening of the paint during the paint-bake process. Alclad 7075 performed better than 7021+ in this regard, which is in line with earlier findings on improving the paint-bake–response of AA7075 by pre-ageing [5–7]. However, cladded sheet may be too expensive for automotive use and the high Cu content of AA7075 may not be acceptable for car manufacturers due to corrosion concerns: although SCC behavior is generally better for Cu-containing 7xxx series alloys, other corrosion forms such as pitting or exfoliation corrosion are worse than in low-Cu alloys [28]. The 7021+ alloy, on the other hand, has a much lower Cu content and may be more readily adoptable. It is suitable for fusion-welding and SCC can be well controlled [29]. In addition, the formability of 7021+ was better so it could be formed at a lower temperature of 120 °C (vs. 160 °C), which may be preferable in an industrial context.

For uses that do not rely on paint-bake, the short-T6 treatment in combination with warm-forming may be used. It yields mechanical properties closer to T6 for both investigated alloys. For warm-forming, we relied entirely on standard oil-based lubricants which are more economical than special lubricants for high temperatures. This is an important advantage of warm-forming at lower temperatures over high-temperature processes such as hot stamping. W-temper forming at RT, on the other hand, can suffer from springback [30].

4. Conclusions

We performed deep-drawing experiments at temperatures of 120 and 160 °C using a high-Cu and a low-Cu Al–Zn–Mg alloy in under-aged temper. Then, ageing was completed either by a simulated single-step paint-bake treatment or a longer

treatment termed short-T6 (160 °C, 130 min). The mechanical properties were assessed and compared to T6 sheet by tensile testing. Furthermore, hardening precipitates were studied using DSC and STEM.

The following conclusions can be drawn:

- Deep-drawing of pre-aged Al–Zn–Mg(–Cu) sheet at low temperatures (well under 200 °C) using oil-based lubricant is a viable route to produce parts of considerable complexity.
- For both alloys, the short-T6 route with intermediate warm-forming yields strength close to T6 at the expense of roughly −15% in elongation at break.
- The distribution of hardening precipitates in the 7021+ alloy after the short-T6 treatment is coarser than in T6 state, but finer than in the paint-baked condition. These findings correlate well with DSC measurements and tensile testing.

Data availability statement

The data that support the findings of this study are available upon reasonable request from the corresponding author.

Declaration of Competing Interest

The authors declare that they have no known competing financial interests or personal relationships that could have appeared to influence the work reported in this paper.

Acknowledgments

We thank AMAG rolling GmbH for providing 70721+ free of charge. We thank the technical staff at LKR and Montanuniversitaet Leoben for their assistance. We are grateful to the European Research Council (ERC) for funding this research through Horizon 2020 action via supporting the "TRANSDESIGN" project, number 757961, and to the Austrian Research Promotion Agency (FFG) for funding in the project AMALFI (FFG-No. 872641). The electron-microscopy facility was supported by the FFG in the project 3DnanoAnalytics (FFG-No. 858040). The funding sources had no involvement in study design nor in the collection, analysis and interpretation of data.

REFERENCES

[1] Heat treating of aluminum alloys," in ASM handbook, vol. 4: Heat Treating, pp. 841–879.
[2] Wolverton C. "Crystal structure and stability of complex precipitate phases in Al–Cu–Mg–(Si) and Al–Zn–Mg alloys. Acta Mater 2001;49(16):3129–42. https://doi.org/10.1016/S1359-6454(01)00229-4.
[3] Li J, Peng Z, Li C, Jia Z, Chen W, Zheng Z. Mechanical properties, corrosion behaviors and microstructures of 7075 aluminium alloy with various aging treatments. Trans Nonferrous Metals Soc China 2008;18(4):755–62. https://doi.org/10.1016/S1003-6326(08)60130-2.
[4] Österreicher JA, et al. Warm-forming of pre-aged Al-Zn-Mg-Cu alloy sheet. Mater Des 2020;193:108837. https://doi.org/10.1016/j.matdes.2020.108837.
[5] Omer K, et al. Process parameters for hot stamping of AA7075 and D-7xxx to achieve high performance aged products. J Mater Process Technol 2018;257:170–9. https://doi.org/10.1016/j.jmatprotec.2018.02.039.
[6] Österreicher JA, Kirov G, Gerstl SS, Mukeli E, Grabner F, Kumar M. Stabilization of 7xxx aluminium alloys. J Alloys Compd 2018;740:167–73. https://doi.org/10.1016/j.jallcom.2018.01.003.
[7] Lee Y-S, Koh D-H, Kim H-W, Ahn Y-S. Improved bake-hardening response of Al-Zn-Mg-Cu alloy through pre-aging treatment. Scr. Mater. 2018;147:45–9. https://doi.org/10.1016/j.scriptamat.2017.12.030.
[8] Stemper L, et al. Giant hardening response in AlMgZn(Cu) alloys. Acta Mater 2021;206:116617. https://doi.org/10.1016/j.actamat.2020.116617.
[9] Azarniya A, Taheri AK, Taheri KK. Recent advances in ageing of 7xxx series aluminum alloys: a physical metallurgy perspective. J Alloys Compd 2019;781:945–83. https://doi.org/10.1016/j.jallcom.2018.11.286.
[10] Sha G, Cerezo A. "Early-stage precipitation in Al–Zn–Mg–Cu alloy (7050). Acta Mater 2004;52(15):4503–16. https://doi.org/10.1016/j.actamat.2004.06.025.
[11] Harrison NR, Luckey SG, Cappuccilli B, Kridli G. Paint bake influence on AA7075 and AA7085. SAE Technical Paper; 2017.
[12] Wan L, Deng Y-L, Ye L-Y, Zhang Y. The natural ageing effect on pre-ageing kinetics of Al-Zn-Mg alloy. J Alloys Compd 2019;776:469–74. https://doi.org/10.1016/j.jallcom.2018.10.338.
[13] Zhao J, Liu Z, Bai S, Zeng D, Luo L, Wang J. "Effects of natural aging on the formation and strengthening effect of G.P. zones in a retrogression and re-aged Al–Zn–Mg–Cu alloy. J Alloys Compd 2020;829. https://doi.org/10.1016/j.jallcom.2020.154469. 154469.
[14] Osten J, Milkereit B, Schick C, Kessler O. "Dissolution and precipitation behaviour during continuous heating of Al–Mg–Si alloys in a wide range of heating rates. Materials 2015;8(5):2830–48. https://doi.org/10.3390/ma8052830.
[15] Grabner F, et al. Cryogenic forming of Al-Mg alloy sheet for car outer body applications. Adv Eng Mater 2019;21(8). https://doi.org/10.1002/adem.201900089. 1900089.
[16] Falkinger G, Sotirov N, Simon P. An investigation of modelling approaches for material instability of aluminum sheet metal using the GISSMO-model," presented at the 10th European LS-DYNA Conference. Germany: Würzburg; 2015.
[17] Deschamps A, Bréchet Y, Livet F. "Influence of copper addition on precipitation kinetics and hardening in Al–Zn–Mg alloy. Mater Sci Technol 1999;15(9):993–1000. https://doi.org/10.1179/026708399101506832.
[18] Cao C, Zhang D, Wang X, Ma Q, Zhuang L, Zhang J. Effects of Cu addition on the precipitation hardening response and intergranular corrosion of Al-5.2Mg-2.0Zn (wt.%) alloy. Mater Char 2016;122:177–82. https://doi.org/10.1016/j.matchar.2016.11.004.
[19] Chinh NQ, Lendvai J, Ping DH, Hono K. "The effect of Cu on mechanical and precipitation properties of Al–Zn–Mg alloys. J Alloys Compd 2004;378(1):52–60. https://doi.org/10.1016/j.jallcom.2003.11.175.
[20] Lloyd DJ, Chaturvedi MC. A calorimetric study of aluminium alloy AA-7075. J Mater Sci 1982;17(6):1819–24. https://doi.org/10.1007/BF00540811.
[21] Chemingui M, Ameur R, Optasanu V, Khitouni M. "DSC analysis of phase transformations during precipitation

hardening in Al–Zn–Mg alloy (7020). J Therm Anal Calorim 2019;136:1887–94. https://doi.org/10.1007/s10973-018-7856-9.
[22] Tang J, et al. Influence of quench-induced precipitation on aging behavior of Al-Zn-Mg-Cu alloy. Trans Nonferrous Metals Soc China 2012;22(6):1255–63. https://doi.org/10.1016/S1003-6326(11)61313-7.
[23] Shu WX, et al. "Tailored Mg and Cu contents affecting the microstructures and mechanical properties of high-strength Al–Zn–Mg–Cu alloys. Mater Sci Eng, A 2016;657:269–83. https://doi.org/10.1016/j.msea.2016.01.039.
[24] Park JK, Ardell AJ. Correlation between microstructure and calorimetric behavior of aluminum alloy 7075 and Al–Zn–Mg alloys in various tempers. Mater Sci Eng, A 1989;114:197–203. https://doi.org/10.1016/0921-5093(89)90859-9.
[25] Gladman T. Precipitation hardening in metals. Mater Sci Technol 1999;15(1):30–6. https://doi.org/10.1179/026708399773002782.
[26] Poole WJ, Wang X, Lloyd DJ, Embury JD. "The shearable–non-shearable transition in Al–Mg–Si–Cu precipitation hardening alloys: implications on the distribution of slip, work hardening and fracture. Philos Mag 2005;85(26–27):3113–35. https://doi.org/10.1080/14786430500154935.
[27] Chinh Nguyen Q, Kovács Zsolt, Reich L, Székely F, Illy Judit, Lendvai Janos. Precipitation and work hardening in high strength AlZnMg(Cu,Zr) alloys. Mater Sci Forum May 1996;217–222:1293–8. https://doi.org/10.4028/www.scientific.net/MSF.217-222.1293.
[28] Yuan D, et al. Enhancing stress corrosion cracking resistance of low Cu-containing Al-Zn-Mg-Cu alloys by slow quench rate. Mater Des 2019;164:107558. https://doi.org/10.1016/j.matdes.2018.107558.
[29] Grohmann T. "Forming of AMAG 7xxx series aluminium sheet alloys," presented at New developments in sheet metal forming. Germany: Fellbach; 2016.
[30] Schuster PA, Österreicher JA, Kirov G, Sommitsch C, Kessler O, Mukeli E. Characterisation and comparison of process chains for producing automotive structural parts from 7xxx aluminium sheets. Metals 2019;9(3):305. https://doi.org/10.3390/met9030305.